MENU 2007
11th International Conference
on Meson-Nucleon Physics and
the Structure of the Nucleon
September10-14, 2007
IKP, Forschungzentrum Jülich, Germany

NEW RESULTS ON THE RARE DECAY $\eta \to \pi^0\gamma\gamma$

S. Prakhov (for the Crystal Ball Collaboration at AGS and the Crystal Ball Collaboration at MAMI) [1]
Department of Physics and Astronomy
University of California, Los Angeles
BOX 951547, Los Angeles, California 90095-1547, USA

Abstract

New results on the rare, doubly-radiative decay $\eta \to \pi^0\gamma\gamma$ have been obtained from a reanalysis of the Crystal Ball experiment performed at the AGS and the first analysis of a recent Crystal Ball experiment at MAMI-B. The analyses have yielded the first results on the dependence of the decay width on the two-photon invariant mass squared, $d\Gamma(\eta \to \pi^0\gamma\gamma)/dm^2(\gamma\gamma)$. The new values for the full decay width are: $\Gamma(\eta \to \pi^0\gamma\gamma) = 0.285 \pm 0.031_{\rm stat} \pm 0.049_{\rm syst}$ eV for the AGS reanalysis, and $\Gamma(\eta \to \pi^0\gamma\gamma) = 0.290 \pm 0.059_{\rm stat} \pm 0.022_{\rm syst}$ eV for the MAMI experiment. The results of the AGS and MAMI measurements are in good agreement with each other, and they are close to the calculations of Chiral Perturbation Theory assuming vector-meson dominance.

1 Introduction

The rare, doubly-radiative decay

$$\eta \to \pi^0\gamma\gamma \tag{1}$$

is attracting much attention as there are large uncertainties in its experimental measurements and in calculations that are based on Chiral Perturbation Theory (χPTh).

The experimental challenges in measuring $\eta \to \pi^0\gamma\gamma$ are formidable because of the smallness of doubly-radiative processes, which is typically of order $\alpha^2 = 1/137^2$. Major backgrounds, which can mimic $\eta \to \pi^0\gamma\gamma$ events, come from $\eta \to 3\pi^0$ decays with overlapping photon showers and $\eta \to \gamma\gamma$ decays with split-off showers. Since $BR(\eta \to 3\pi^0) = 0.325$ and

[1] E-mail: prakhov@bmkn8.physics.ucla.edu

$BR(\eta \to \gamma\gamma) = 0.394$, the background from these η decay modes is very significant. Another large background, which also needs to be suppressed, comes from $\pi^0\pi^0$ production.

The uncertainties in χPTh calculations of the $\eta \to \pi^0\gamma\gamma$ decay amplitude are related to the fact that the leading $\mathcal{O}(\mathsf{p}^2)$ term and the $\mathcal{O}(\mathsf{p}^4)$ tree contribution are absent because neither π^0 nor η can emit a photon. Very small contributions come from the $\mathcal{O}(\mathsf{p}^4)$ pion and kaon loops as they are greatly suppressed by G-parity invariance and the large mass of kaons, respectively. The main contribution to the $\eta \to \pi^0\gamma\gamma$ decay amplitude comes from the $\mathcal{O}(\mathsf{p}^6)$ counterterms that are needed in χPTh to cancel various divergences. However, the coefficients of these counterterms are not determined by χPTh itself and depend on the model used for the calculations. Since any χPTh calculation yields the decay amplitude and width, a reliable experimental measurement of the $\eta \to \pi^0\gamma\gamma$ branching ratio and Dalitz plot is important for testing χPTh calculations and the determination of the coefficients for the $\mathcal{O}(\mathsf{p}^6)$ counterterms.

Early attempts to measure and calculate the $\eta \to \pi^0\gamma\gamma$ decay have been reviewed in Ref. [1]. An experimental break-through was achieved in 1981 with the GAMS experiment [2,3], which used a wall of 1400 Cerenkov counters that provided good energy and spatial resolution for high-energy photons. 6×10^5 η mesons were produced in reaction $\pi^- p \to \eta n$, improving the statistics compared to previous experiments by two orders of magnitude. A narrow peak of 40 events in the $\pi^0\gamma\gamma$ invariant-mass spectrum located at the mass value of the η meson was interpreted as the $\eta \to \pi^0\gamma\gamma$ signal. Much attention was paid to suppressing the $\eta \to 3\pi^0$ background. For two decades, the GAMS result, $\Gamma(\eta \to \pi^0\gamma\gamma) = 0.84 \pm 0.17$ eV [3], was the favored experimental value for this decay width. It brought much interest to theoretical calculations that were trying to reproduce the surprisingly large $\eta \to \pi^0\gamma\gamma$ decay width. According to [4–7], the χPTh calculations, which were based on vector-meson dominance (VMD) with additional contributions like scalar, tensor, C-odd axial-vector resonances and other smaller ones, give about half of the GAMS value. Only the calculations using quark-box diagrams [8, 9] got close to the experimental value for $\Gamma(\eta \to \pi^0\gamma\gamma)$.

After 2001 the experimental situation for measuring the $\eta \to \pi^0\gamma\gamma$ decay changed greatly. New experiments reported decay-width values which were two to three times smaller than the GAMS result and were in better agreement with χPTh calculations. The Crystal Ball (CB) collaboration at the AGS conducted an experiment devoted to investigations of rare η-meson decays with a total of 2.8×10^7 η mesons produced in reaction $\pi^- p \to \eta n$ near threshold [10–12], which ended up with $\Gamma(\eta \to \pi^0\gamma\gamma) = 0.45 \pm 0.12$ eV. An independent analysis [13] of the same CB data yielded the relative branching

ratio $B_1 = (8.3 \pm 2.8_{\rm stat} \pm 1.4_{\rm syst}) \times 10^{-4}$ with respect to $BR(\eta \to 3\pi^0)$, this implies $\Gamma(\eta \to \pi^0\gamma\gamma) = 0.35 \pm 0.13$ eV. Meanwhile, the SND collaboration at VEPP-2M reported $\Gamma(\eta \to \pi^0\gamma\gamma) = 0.27^{+0.49}_{-0.25}$ eV [1]. However, their signal was just $7.0^{+12.9}_{-6.5}$ events. Most recent χPTh calculations of $\Gamma(\eta \to \pi^0\gamma\gamma)$, which revised earlier ones, resulted in 0.47 ± 0.10 eV [14] and 0.45—0.53 eV [15], showing good agreement with the new experimental values.

Surprisingly low, in comparison with all earlier measurements and χPTh calculations, is the recent result of the KLOE collaboration [16], $\Gamma(\eta \to \pi^0\gamma\gamma) = 0.108 \pm 0.035_{\rm stat} \pm 0.029_{\rm syst}$ eV, which is based on a signal of 68 ± 23 events. Hypothetically, such a small decay width could be the result of destructive interference between the vector-meson and other meson contributions. To check this experimentally, one should also measure the $\eta \to \pi^0\gamma\gamma$ Dalitz plot, the density of which reflects the decay amplitude. Instead of a Dalitz plot, χPTh calculations usually depict the $d\Gamma(\eta \to \pi^0\gamma\gamma)$ dependence on the invariant mass (or the invariant mass squared) of the two photons from the $\eta \to \pi^0\gamma\gamma$ decay. In Fig. 1, we illustrate the predictions for both the $m(\gamma\gamma)$ and $m^2(\gamma\gamma)$ spectra, which are obtained from the decay amplitudes described in detail in Refs. [5, 8]. The prediction based only on the vector-

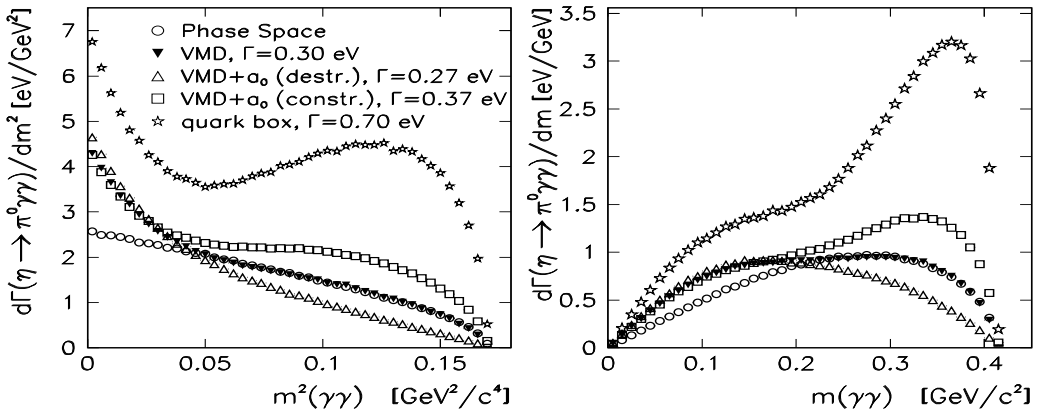

Figure 1: Comparison of different χPTh calculations of Refs. [5, 8] for the dependence of the $\eta \to \pi^0\gamma\gamma$ decay width on $m^2(\gamma\gamma)$ (left) and on $m(\gamma\gamma)$ (right).

meson contribution gives the basic decay width and two-photon invariant-mass spectrum, which is close to phase space when $m^2(\gamma\gamma) > 0.05$ GeV$^2/c^4$. Note that the "pure" VMD prediction for $d\Gamma(\eta \to \pi^0\gamma\gamma)/dm(\gamma\gamma)$ is very similar for most of the existing calculations [4–7, 14]. Adding other contributions to the vector-meson part, for example a_0-meson exchange, changes the decay width and the invariant-mass spectrum depending on the sign of the

interference term. As shown in Fig. 1, there is a typical correlation between the change of the decay width and the change in the two-photon invariant-mass spectrum. Evidently, increasing the total decay width occurs mostly due to the rise in the $d\Gamma(\eta \to \pi^0\gamma\gamma)$ spectrum at high $m(\gamma\gamma)$ masses.

In light of the above, an experimental measurement of the $d\Gamma(\eta \to \pi^0\gamma\gamma)/dm(\gamma\gamma)$ distribution is needed as it provides a unique test of χPTh calculations and the information necessary for the determining the coefficients of the $\mathcal{O}(\mathsf{p}^6)$ counterterms.

In this conference proceeding, we present the first results for the $d\Gamma(\eta \to \pi^0\gamma\gamma)/dm^2(\gamma\gamma)$ distribution and a new value for the $\eta \to \pi^0\gamma\gamma$ branching ratio.

2 Experimental arrangements

The experiments at the AGS (in 1998) and at MAMI (in 2004) were performed with the Crystal Ball multiphoton spectrometer which consists of 672 optically isolated NaI(Tl) crystals that are arranged in two hemispheres covering 93% of 4π steradians. Details about the CB detector at the AGS and the analyses of its data can be found in Refs. [17–19]. Details of measuring $\eta \to \pi^0\gamma\gamma$ at the AGS are given in Ref. [12]. The reanalysis of these data mostly revised the fitting procedure of the experimental distrubutions that allowed obtaining the $d\Gamma(\eta \to \pi^0\gamma\gamma)/dm^2(\gamma\gamma)$ distribution and an improved value for $BR(\eta \to \pi^0\gamma\gamma)$.

The AGS experiment used a momentum-analyzed beam of negative pions incident on a 10-cm-long liquid hydrogen (LH_2) target located in the center of the CB. The mean value of the incident momentum spectrum at the center of the LH_2 target was 716 MeV/c (that is just above the $\pi^-p \to \eta n$ threshold), the momentum spread was $\sim$ 12 MeV/c, and the momentum resolution of an individual beam particle was $\sim$ 0.6%. The number of $\pi^-p \to \eta n$ events produced in our experiment was determined using the $\eta \to \gamma\gamma$ decay mode and equals $(27.64 \pm 0.19) \times 10^6$. The quality of the data analysis and Monte Carlo (MC) simulation is illustrated in Ref. [12].

In our analysis of the AGS data, we searched for the process $\pi^-p \to \eta n \to \pi^0\gamma\gamma n \to 4\gamma n$ in four-cluster events, assuming that all clusters in the CB were produced by the electromagnetic showers of the final-state photons. The neutron was analyzed as being the missing particle. Since the $\pi^-p \to \eta n$ reaction was measured near the production threshold where the majority of the final-state neutrons left through the downstream tunnel of the CB, the fraction of the η events with the neutron detected in the CB comprised only 5%.

The experiment at MAMI was conducted with the beam of Bremsstrahlung photons from MAMI-B (multistage electron accelerator with maximum energy of ~ 883 MeV) that were incident on a 5-cm-long LH_2 target located in the center of the CB. To cover the exit beam tunnel of the CB, the TAPS photon detector [20] was installed 1.75 m downstream of the CB center. In this experiment, TAPS consisted of 510 individual BaF_2 detectors that are hexagonally shaped with an inner diameter of 6 cm and a length of 25 cm (corresponding to 12 radiation lengths). The typical energy resolution for electromagnetic showers in TAPS is $\Delta E/E = 0.018 + 0.008/(E[\text{GeV}])^{0.5}$. Due to the long distance between the CB and TAPS, the resolution of TAPS in the polar angle θ was better than 1°. The resolution in azimuthal angle ϕ is better than $1/R$ radian, where R is the distance in [cm] from the TAPS center to the point on the TAPS surface corresponding to the θ angle. The incident photons were tagged with the Bremsstrahlung recoil electrons detected by the Tagger spectrometer. The Tagger consisted of a momentum-dispersed magnet [21] focusing the electrons on the focal plane detector of 353 half-overlapping plastic scintillators [22]. The energy resolution of the tagged photon beam, which is defined by the overlap region of two scintillation counters, is about 1 MeV. The maximum energy for tagging the beam photon with the Tagger was 820 MeV.

In the analysis of the MAMI data, we searched for the process $\gamma p \to \eta p \to \pi^0\gamma\gamma p \to 4\gamma p$ in events with five clusters detected in the CB and TAPS in coincidence with the prompt signal from the Tagger. The detection of the recoil proton was required to improve the experimental resolution and the signal-to-background ratio compared to the AGS-data analysis. The number of the $\eta \to \gamma\gamma$ decays observed was based on $\sim 10^7$ $\gamma p \to \eta p$ events produced in the experiment. More details on the experimental set-up and data analysis can be found in Ref. [23].

3 Selection of the $\eta \to \pi^0\gamma\gamma$ candidates

The search for a signal from the $\eta \to \pi^0\gamma\gamma$ decays is similar for the AGS and MAMI data. The signal should be seen as a peak in the invariant-mass spectrum of the $\pi^0\gamma\gamma$ final state at the position corresponding to the η-meson mass value. This means that one has to search for process $\pi^- p \to \pi^0\gamma\gamma n \to 4\gamma n$ in the AGS data and process $\gamma p \to \pi^0\gamma\gamma p \to 4\gamma p$ in the MAMI data. Since the major contribution to the four-photon final states comes from direct $\pi^0\pi^0$ production, this reaction must be suppressed in our analysis. The kinematic-fitting technique was used for testing hypotheses on the necessary processes and selecting event candidates based on the fit

confidence level (CL). The $\pi^0\pi^0$ background was suppressed by discarding all events that satisfied the $\pi^0\pi^0$ hypothesis with probability greater than 0.001%. Further suppression of the background processes can be done by requiring a cut on the confidence level of the $\pi^0\gamma\gamma$ hypothesis itself. Our typical cut on this was at the 10% CL (i.e., with a probability greater than 10%). Besides the "smooth" background from the $\pi^0\pi^0$ production in the $m(\pi^0\gamma\gamma)$ spectrum, there are contributions from other neutral η decays that can mimic the $\eta \to \pi^0\gamma\gamma$ signal. The $\eta \to 3\pi^0$ decay produces four clusters because of overlapping photon showers and the $\eta \to \gamma\gamma$ decay does the same because of split-off showers. The kinematic-fit cuts on CL are not enough for sufficient suppression of these background contributions. As illustrated in Ref. [12], further suppression of the $\eta \to \gamma\gamma$ and $\pi^0\pi^0$ background contributions can be reached by applying a cut on $m(\pi^0\gamma)$ with respect to $m(\pi^0\gamma\gamma)$. The overlapping clusters can be partially separated from the normal single-photon ones by testing their radius as a function of the cluster energy. The

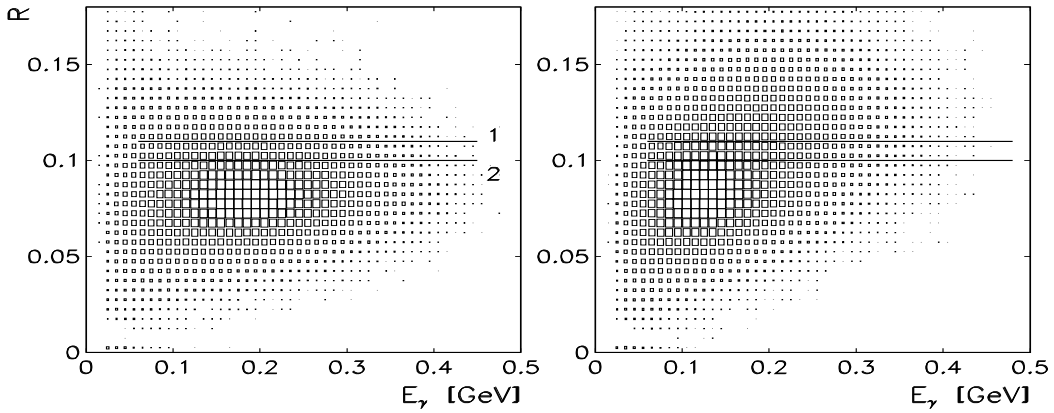

Figure 2: Two-dimensional distributions of the effective cluster radius R versus the cluster energy of the photons for events selected as $\pi^- p \to \pi^0\gamma\gamma n$ candidates: (left) MC simulation for $\pi^- p \to \eta n \to \pi^0\gamma\gamma n$, (right) MC for $\pi^- p \to \eta n \to 3\pi^0 n$. The lines in the distributions show the cuts on R. The cuts require discarding all events for which a cluster energy is greater than 0.06 GeV and R is above the line. Cut #2 is tighter than #1.

so-called effective radius R of a cluster containing k crystals with energy E_i deposited in crystal i is defined as $R = \sqrt{\sum_i^k E_i \cdot (\Delta r_i)^2 / \sum_i^k E_i}$, where Δr_i is the opening angle (in radians) between the cluster direction and the crystal axis. As seen in Fig. 2, the cluster radii for the $\eta \to 3\pi^0$ background events are systematically larger compared to the ones for $\eta \to \pi^0\gamma\gamma$ events.

Since the length of the LH_2 targets was not insignificant, we could improve the angular resolution using the z coordinate of the event vertex as a free parameter in the kinematic fit. For background reactions, the resulting z-coordinate distribution does not correspond to the real vertex distribution. Thus applying a cut on the z coordinate, which was obtained from the kinematic-fit output, allowed further improvement of the signal-to-background ratio.

The typical acceptance for $\eta \to \gamma\gamma$ events after applying our standard selection criteria was about 15% for the AGS-data analysis and 8% for MAMI-B. A lower acceptance for MAMI-B is due to the requirement that the recoil proton must be detected. Note also that the detection efficiency for the recoil protons is smaller than for the photons, as low energy protons do stop in the material located between the target and the crystals.

4 Determination of $d\Gamma(\eta \to \pi^0\gamma\gamma)/dm^2(\gamma\gamma)$

To determined the $d\Gamma(\eta \to \pi^0\gamma\gamma)/dm^2(\gamma\gamma)$ spectrum, we divided our experimental and MC-simulated data in seven subsamples depending on the $m^2(\gamma\gamma)$ value, which was obtained as a result of testing the $\pi^0\gamma\gamma$ hypothesis. Then, from the experimental spectra of $m(\pi^0\gamma\gamma)$, we subtracted the background spectra from the MC simulation of the $\eta \to 3\pi^0$ and $\eta \to \gamma\gamma$ events. The fraction of these remaining backgrounds, which depends on the selection cuts used, was determined from the ratio of the number of these η decays observed in the experiment itself to the number of events generated for these decays in our MC simulation. The resulting $m(\pi^0\gamma\gamma)$ spectra were fitted to a smooth polynomial function for the remaining background plus a Gaussian for the expected signal. The initial parameters for the polynomial function were determined from the fit of the MC simulation for the $\pi^0\pi^0$ background; the mean value and sigma for the Gaussian were fixed according to the fit of the MC simulation for the $\eta \to \pi^0\gamma\gamma$ events. Examples of the fits of some $m^2(\gamma\gamma)$ ranges are illustrated in Fig. 3 for both the AGS and MAMI-B data. Note that the MAMI-B spectra have smaller statistics but better signal-to-background ratios.

The results on the $\eta \to \pi^0\gamma\gamma$ decay width as a function of $m^2(\gamma\gamma)$ are shown in Fig. 4 for both the AGS and MAMI-B data. The analysis was repeated several times using different criteria for event selection. In order to illustrate the variation of results in each $m^2(\gamma\gamma)$ interval, they are all plotted in the same Figure. The acceptance in each $m^2(\gamma\gamma)$ interval was determined using the phase-space simulation of the $\eta \to \pi^0\gamma\gamma$ decay. The decay-width calculation was based on the experimental ratio of the $\eta \to \pi^0\gamma\gamma$

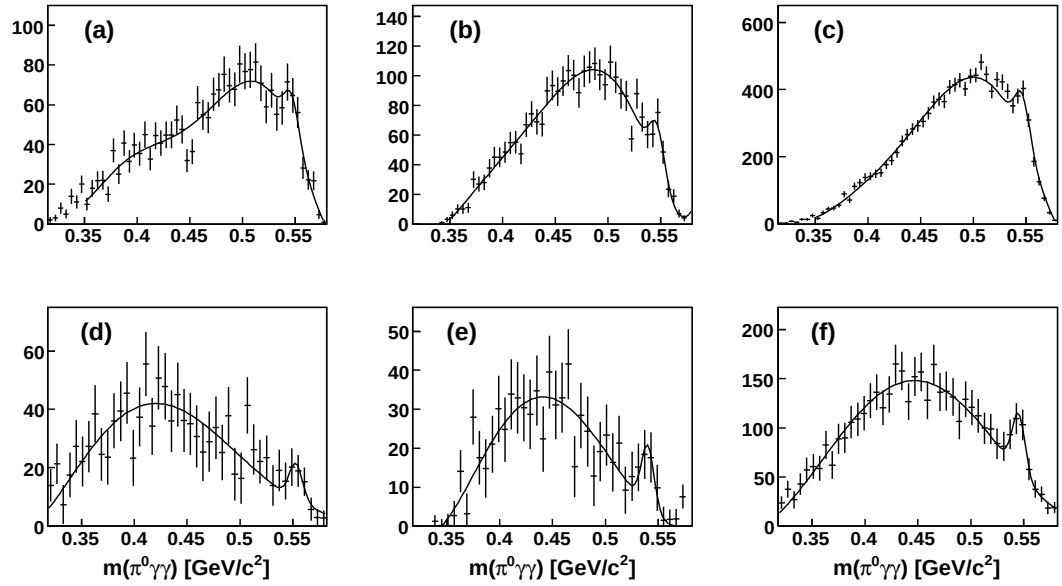

Figure 3: Fit of the $m(\pi^0\gamma\gamma)$ spectra for the AGS (top) and MAMI-B (bottom): (a,d) $0.027 < m^2(\gamma\gamma) < 0.04$ GeV$^2/c^4$; (b,e) $0.04 < m^2(\gamma\gamma) < 0.06$ GeV$^2/c^4$; (c,f) full $m^2(\gamma\gamma)$.

and $\eta \to 3\pi^0$ events measured, and using the branching ratio for $\eta \to 3\pi^0$ and the full width $\Gamma(\eta \to \text{all}) = 1.29 \pm 0.07$ keV from the latest edition of the Review of Particle Physics [24]. In Fig. 4, we also depict the VMD prediction for the $d\Gamma(\eta \to \pi^0\gamma\gamma)/dm^2(\gamma\gamma)$ distribution based on the calculations of Ref. [5]. This VMD prediction matches our results better if we normalize it to $\Gamma(\eta \to \pi^0\gamma\gamma) = 0.33$ eV for the AGS results and to 0.37 eV for MAMI-B. Our results are in reasonable agreement with χPTh predictions based on the vector-meson contribution only. However, we do not pretend that other contributions are absent. So, to enable one to fit our results to other models, we calculated the average of the results for $d\Gamma(\eta \to \pi^0\gamma\gamma)/dm^2(\gamma\gamma)$ in each $m^2(\gamma\gamma)$ interval and listed them in Table 1. Note that the $m^2(\gamma\gamma)$ range between 0.011 and 0.027 GeV$^2/c^4$ is absent because of zero acceptance after the suppression of the $\pi^0\pi^0$ background. Since the measurements with different selection criteria are correlated, the uncertainties of the values were calculated by adding in quadrature the average of the individual errors in each $m^2(\gamma\gamma)$ interval and the r.m.s. of the results themselves. Note that the AGS results for the $d\Gamma(\eta \to \pi^0\gamma\gamma)/dm^2(\gamma\gamma)$ distribution are in agreement within the error bars with the MAMI-B results. More precise measurements of this distribution require significantly higher experimental statistics, which is expected from the CB experiments at MAMI-C. On the other hand, as seen

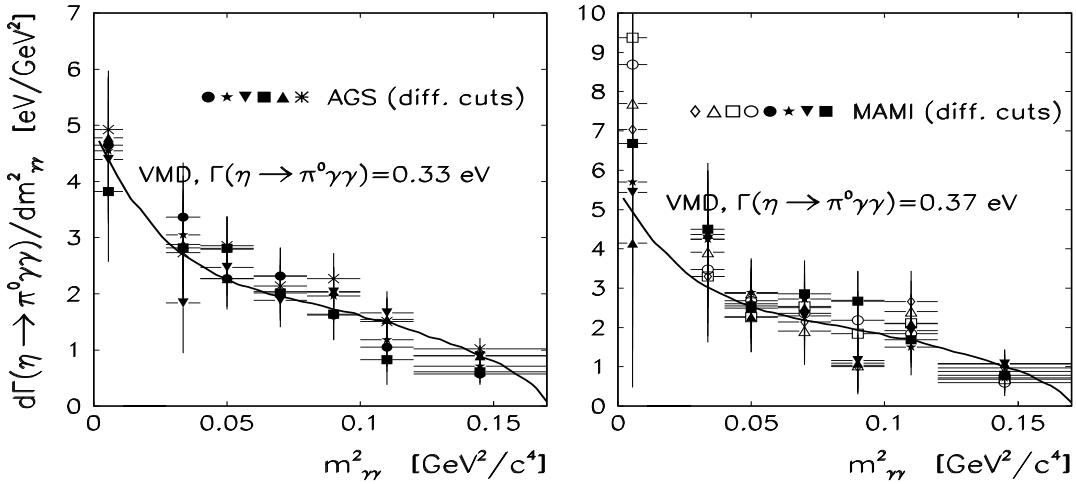

Figure 4: The $d\Gamma(\eta \to \pi^0\gamma\gamma)/dm^2(\gamma\gamma)$ results obtained for different selection criteria of the AGS (left) and MAMI-B (right) data. The VMD prediction (solid line) is calculated according to Ref. [5] and normalized to $\Gamma(\eta \to \pi^0\gamma\gamma) = 0.33$ eV for the AGS results and to 0.37 eV for MAMI-B.

Table 1: The $d\Gamma(\eta \to \pi^0\gamma\gamma)/dm^2(\gamma\gamma)$ results (in units [eV/GeV^2]) for seven intervals of $m^2(\gamma\gamma)$ calculated from the average of the measurements shown in Figs. 4.

$m^2(\gamma\gamma)$ [GeV$^2/c^4$]	0.—0.011	0.027—0.04	0.04—0.06	0.06—0.08
$d\Gamma/dm^2(\gamma\gamma)$ (AGS)	4.5 ± 1.2	2.8 ± 1.1	2.58 ± 0.59	2.12 ± 0.51
$d\Gamma/dm^2(\gamma\gamma)$ (MAMI)	6.8 ± 4.0	3.9 ± 1.6	2.58 ± 0.90	2.41 ± 0.90
$m^2(\gamma\gamma)$ [GeV$^2/c^4$]	0.08—0.1	0.1—0.12	0.12—0.17	
$d\Gamma/dm^2(\gamma\gamma)$ (AGS)	1.93 ± 0.51	1.30 ± 0.52	0.78 ± 0.25	
$d\Gamma/dm^2(\gamma\gamma)$ (MAMI)	1.71 ± 1.00	2.03 ± 0.83	0.85 ± 0.39	

from the fits of our samples to the full $m^2(\gamma\gamma)$ range (shown in Figs. 3(c,f)), the present statistics are high enough for the determination of the full decay width for $\eta \to \pi^0\gamma\gamma$. Based on our $d\Gamma(\eta \to \pi^0\gamma\gamma)/dm^2(\gamma\gamma)$ results, we simulated the $\eta \to \pi^0\gamma\gamma$ decay according to the VMD amplitude of Ref. [5], and used this Monte Carlo simulation for the determination of our overall acceptance. The average of our results from the fits to our $m(\pi^0\gamma\gamma)$ spectra, which were obtained for different selection criteria, yielded for the AGS and MAMI-B analyses

$$BR_{\rm AGS}(\eta \to \pi^0\gamma\gamma) = (2.21 \pm 0.24_{\rm stat} \pm 0.38_{\rm syst}) \times 10^{-4} = (2.21 \pm 0.45_{\rm tot}) \times 10^{-4} \ ,$$
$$BR_{\rm MAMI-B}(\eta \to \pi^0\gamma\gamma) = (2.25 \pm 0.46_{\rm stat} \pm 0.17_{\rm syst}) \times 10^{-4} = (2.25 \pm 0.49_{\rm tot}) \times 10^{-4} \ .$$

By the "statistical" uncertainty, we mean the average uncertainty based on the fit errors; the systematic uncertainty comes from the r.m.s. of all results obtained for different selection criteria. The corresponding values for the decay width are

$$\Gamma_{\rm AGS}(\eta \to \pi^0\gamma\gamma) = 0.285 \pm 0.031_{\rm stat} \pm 0.049_{\rm syst} = 0.285 \pm 0.058_{\rm tot}\ {\rm eV},$$
$$\Gamma_{\rm MAMI-B}(\eta \to \pi^0\gamma\gamma) = 0.290 \pm 0.059_{\rm stat} \pm 0.022_{\rm syst} = 0.290 \pm 0.063_{\rm tot}\ {\rm eV}.$$

Our new AGS value for the $\eta \to \pi^0\gamma\gamma$ decay width is somewhat smaller than $\Gamma(\eta \to \pi^0\gamma\gamma) = 0.45 \pm 0.12$ eV reported earlier by us in Ref. [12], but both values overlap within the error bars. For the most part, we explain this difference by the uncertainty in the definition of the $\pi^0\pi^0$ background shape under the $\eta \to \pi^0\gamma\gamma$ signal. From the comparison of the previous AGS data analysis with the present one, we have found that a small discrepancy in the shape between the real $\pi^0\pi^0$ background and the MC-simulated one resulted in some gain of the weight factor for the $\eta \to \pi^0\gamma\gamma$ signal spectrum in our binned maximum-likelihood fits. In the new fitting procedure, we fixed only the $\eta \to \pi^0\gamma\gamma$ peak parameters, taking them according to the MC simulation, while the parameters for the $\pi^0\pi^0$ background were free, but initialized from a fit of the $\pi^0\pi^0$ MC simulation. Our new AGS result for $\Gamma(\eta \to \pi^0\gamma\gamma)$ supersedes the results reported earlier in Refs. [10–12].

5 Summary and conclusions

New results on the rare, doubly-radiative decay $\eta \to \pi^0\gamma\gamma$ have been obtained from a reanalysis of the Crystal Ball experiment performed at the AGS and the first analysis of a new Crystal Ball experiment at MAMI-B. The analyses have yielded the first results on the dependence of the decay width on the two-photon invariant mass squared, $d\Gamma(\eta \to \pi^0\gamma\gamma)/dm^2(\gamma\gamma)$, and new values for the $\eta \to \pi^0\gamma\gamma$ branching ratio. The results of the AGS and MAMI measurements are in good agreement with each other, and they are close to the calculations of Chiral Perturbation Theory assuming vector-meson dominance.

All our results that are presented in this conference contribution are close to final, but should still be classified as preliminary.

References

[1] M. M. Achasov *et al.* [SND Collab.], *Nucl. Phys.* **B600**, 3 (2001).

[2] F. Binon *et al.* [GAMS Collab.], *Yad. Fiz.* **33**, 1534 (1982) also *Lett. Nuovo Cim.* **A71**, 497 (1982).

[3] D. Alde *et al.* [GAMS Collab.], *Z. Phys.* **C25**, 225 (1984).

[4] Ll. Ametller, J. Bijnens, A. Bramon and F. Cornet, *Phys. Lett.* **B276**, 185 (1992).

[5] J.N. Ng and D.J. Peters, *Phys. Rev.* **D46**, 5034 (1992).

[6] P. Ko, *Phys. Rev.* **D47**, 3933 (1993).

[7] M. Jetter, *Nucl. Phys.* **B459**, 283 (1996).

[8] J.N. Ng and D.J. Peters, *Phys. Rev.* **D47**, 4939 (1993).

[9] Y. Nemoto, M. Oka, and M. Takizawa, *Phys. Rev.* **D54**, 6777 (1996).

[10] S. Prakhov [for Crystal Ball Collab.], *Phys. of Atom. Nucl.* **65**, 2238 (2002).

[11] B.M.K. Nefkens and J.W. Price, "Eta Physics Handbook" *Physica Scripta* **T99**, 114 (2002).

[12] S. Prakhov *et al.* [Crystal Ball Collab.] *Phys. Rev.* **C72**, 025201 (2005).

[13] N. Knecht *et al.*, *Phys. Lett.* **B589**, 14 (2004).

[14] E. Oset, J.R. Pelaez, and L. Roca, *Phys. Rev.* **D67**, 073013 (2003).

[15] A.E. Radzhabov and M.K. Volkov , *Phys. Rev.* **D74**, 113001 (2006).

[16] B.Di Micco *et al.* [KLOE Collab.], *Acta Phys. Slov.* **56**, 403 (2006).

[17] W. B. Tippens *et al.* [Crystal Ball Collab.] *Phys. Rev. Lett.* **87**, 192001 (2001).

[18] S. Prakhov *et al.* [Crystal Ball Collab.] *Phys. Rev.* **C69**, 045202 (2004).

[19] M.E. Sadler *et al.* [Crystal Ball Collab.] *Phys. Rev.* **C69**, 055206 (2004).

[20] R. Novotny, *IEEE Trans. Nucl. Sci.* **38**, 379 (1991).

[21] I. Anthony *et al.*, *NIM* **A301**, 230 (1991).

[22] S.J. Hall *et al.*, *NIM* **A368**, 698 (1996).

[23] J.W. Brudvik, *Ph.D. Thesis*, University of California Los Angeles(2007).

[24] A. B. Balantekin *et al.* [Particle Data Group], *J. Phys. G: Nucl. Part. Phys.* **33**, 1 (2006).